PHYSICAL REVIEW E **76**, 050401(R) (2007)

Layering transitions in confined colloidal crystals: The hcp-like phase

F. Ramiro-Manzano,[1] E. Bonet,[2] I. Rodriguez,[1] and F. Meseguer[1,*]

[1]*Centro Tecnológico de Ondas–Unidad Asociada CSIC-ICMM/UPV, Universidad Politécnica de Valencia, Avenida Los Naranjos, 46022 Valencia, Spain*

[2]*Departamento de Física Aplicada, Universidad Politécnica de Valencia, Avenida Los Naranjos, 46022 Valencia, Spain*

(Received 8 March 2007; revised manuscript received 31 July 2007; published 6 November 2007)

This paper investigates the sequence of morphological transitions in a nearly hard sphere arrangement confined in a wedge cell. A model that shows smooth transitions between the different particle orderings for a small number of layers is proposed. In this model, both the buckling and the (100) hexagonal close packed (hcp) phases are particular cases of a much more general particle arrangement tendency that we call hcp-like ordering. This phase, which does not correspond to any known close packed ordering, is able to adopt packing arrangements commensurate with the cell thickness. More striking, the hcp-like phase adapts itself to the progressive changes of the cell thickness by a smooth change in the interlayer spacing. We present hcp-like orderings up to six layers and a complete sequence of transformations between two and four layers. Finally, a packing model of the transition from two to three layers is also presented.

DOI: 10.1103/PhysRevE.76.050401 PACS number(s): 82.70.Dd, 61.72.Nn, 64.70.Dv

The process of crystallization in a confined colloidal suspension is very different from the bulk systems [1–3]. When a colloid solution is confined between two plates, only an integer number of crystalline layers may exist in equilibrium, resulting in many different types of layer arrangements. Pieranski *et al.* [1] have studied the sequence of facets when the thickness of the cell gradually increases. They used a wedge cell with nearly hard sphere colloids and the proposed sequence, for a few layers, was basically the following:

$$1\,\triangle \rightarrow 1B \rightarrow 2\,\square \rightarrow 2\mathrm{r} \rightarrow 2\,\triangle \rightarrow 3\,\square \rightarrow 3\,\triangle\,, \quad (1)$$

where $\triangle$ and $\square$ stand for triangular and square layer arrangements corresponding to the (111) and (100) fcc facets. B and r are the buckling and rhombic phases, respectively [4]. More recently, Neser *et al.* [5] introduced the prismatic phase as a buckling mechanism for more than two layers. Other phases from different experiments obtained on wet or dried samples [6–8] have been explained by theoretical simulations [9–13]. Despite all these contributions, a complete mechanism of phase transitions between different particle orderings has not yet been published. The general transition process scheme [1] shows abrupt changes in the packing values when the system changes between different phases. They appear mainly at very small thickness values where only very few layers can be packed. This is a consequence of the adaptation of a finite number of layers to a continuous variation of the gap in the confined wedge geometry. Recently, we have shown smooth transitions between the different particle orderings when the wedge sample is several monolayers thick [14]. Indeed, the colloidal system adapts itself to the continuous variation of wedge thickness by introducing an appropriate number of stacking faults to maximize the filling fraction value.

This Rapid Communication will focus on understanding the structure sequence observed as the sample thickness progressively increases from two to six layers. For this purpose, wedge samples were also employed, since this kind of design allows study of the packing of spheres as a function of the number of layers. As assumed previously, a maximum packing value of touching spheres is still the required condition in the facet ordering. A path over the sample, starting from zero thickness toward increasing thickness value areas, was examined. While the number of monolayers increased, the evolution of the facets in the sample and the transition between them were studied. To allow accurate identification of the different colloidal arrangements, optical experiments as well as scanning electron microscopy (SEM) characterization were performed. We found that the buckling phase in the transition between one and two monolayers can be extended to a larger number of layers. This new phase, which we call hcp-like, is very versatile, as it easily adapts itself to the gap value of the wedge cell. Moreover, we show that hcp-like ordering plays a very important role in smoothing the transition $n\triangle \rightarrow (n+1)\square$ for small values of n.

The design of the cell of the wedge samples has been previously described by Ramiro-Manzano *et al.* [14]. Briefly, our wedge type cells, based on that used by Lu *et al.* [15], are formed by two large plates (3 cm long): a hydrophilic (treated glass) substrate plate and a hydrophobic [polystyrene (PS)] covering plate. In order to achieve a great variety of crystallographic facets and large single crystal areas (of the order of millimeters), we use very small wedge angles ($<10^{-4}$ rad). For this purpose a 6-μm-thick Mylar film, attached along only one rim of the slides, separates the plates. The wedge cell is tightened with several binder clips on the three other sides of the cell. Polystyrene particles of different sizes ranging from 245 up to 800 nm in diameter (Ikerlat Polymers) were employed. Particles were washed and rinsed several times with milli-Q water. A pure aqueous, pH=7, suspension of particles (1 wt %) was introduced through a 2-cm-high glass tube attached to the inner part of the cell through a small hole (2 mm diameter) drilled on the glass plate. Several drops were put into the small tube, which entered the cell due to capillary forces. The particle concentra-

*Corresponding author. fmese@fis.upv.es

tion increased at the same time as water leaked out and evaporated. After about one week, the system condensed into several facets, and, finally, the sample dried. Different facets made of uniform touching hard spheres were obtained.

As the PS slide can be easily detached from the sample with almost no damage to the crystalline structure, very high-quality colloidal crystal thin films are obtained. One can see the different iridescent colors corresponding to the different particle arrangements of the wedge samples. The extension of the crystal arrangements provides information about the stability of the different phases. Through a careful topographical inspection we determine the path over the sample to study the evolution of the particle order as the thickness evolves from one to several monolayers (MLs). By making different marks, we are able to perform optical experiments first, and, then SEM analysis (front and side views) of the zones that have been optically monitored. We have observed the extension of the crystal arrangements and we have considered only those phases with a minimum extension to obtain a reliable optical spectrum.

Optical reflectance spectra were recorded by using a Fourier-transformed infrared IFS-66 Bruker spectrometer coupled to an optical microscope provided with a 15× Cassegrain objective. From optical experiments (and the comparison to SEM data) we can have precise information on both the crystallographic facet ordering (and the corresponding interplanar distance) and the number of monolayers in the thin film colloidal crystal (see details in Ramiro-Manzano *et al.* [14]).

In this Rapid Communication, we concentrate on the transition between 2 and 6 ML, with especial emphasis on both the complete sequence $2\square \rightarrow 4\square$ and also the role of the *n* hcp-like phase in the ordering transitions.

The well-known transition $1\triangle \rightarrow 1B \rightarrow 2\square$ helps us to understand the transition in the next stage of two monolayers. For thickness value equal to the sphere size, maximum packing fraction corresponds to a triangular facet ($1\triangle$). Then, as the height of the confined sample increases, a buckled phase appears. Such a buckling mechanism maximizes the packing fraction between one and two layers [16]. Indeed, one zone with two sublayers is generated, and a two-layer structure begins to be formed ("escape in the third dimension" [1]). By changing the magnitude of the vertical displacement of the sublayers, the buckling phase can easily adapt itself to the gap of the wedge cell, and thus maximize the filling fraction value. We show later that the buckling phase can be considered as a precursor of our proposed hcp-like phase.

(*a*) $2 \rightarrow 3$ *transition*. Figure 1 shows the optical reflectance spectra taken on the path transition between the $2\square$ and $3\square$ facets. We have also included SEM images of the different phases sampled by the light spot. The analysis of their corresponding optical spectra, and the comparison to the SEM images, allows us to make an accurate assignment of the particles arrangement [14].

An analysis of the sample clearly reveals that the transition sequence is in fact $2\square \rightarrow 2\triangle \rightarrow 3\square$ (Fig. 1). It has been extensively reported, both experimentally [4,8] and theoretically [9,13], that the $2\square \rightarrow 2\triangle$ transition is performed throughout the rhombic phase. As the interlayer separation of

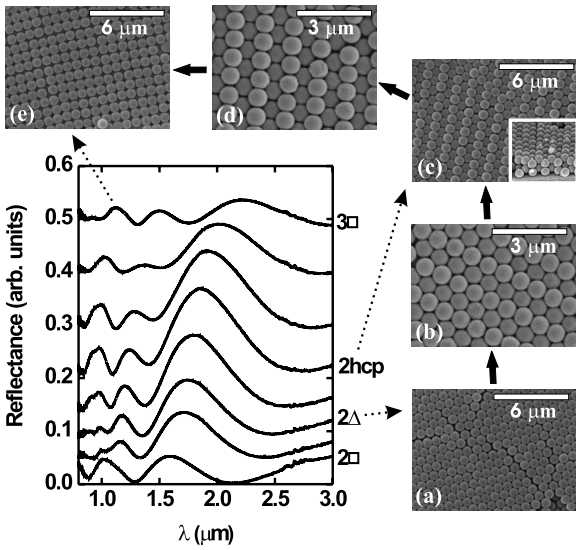

FIG. 1. Reflectance optical spectra obtained over a path in the sample for the transition between $2\square$ and $3\square$, the sphere diameter being $\Phi = 800$ nm. Spectra have been shifted for the sake of comparison. There is a continuous transition, as the displacement of the maximum peak shows. SEM images of the sequence of the different facets: (a) $2\triangle$, (b) hcp-like with $\delta/\Phi \approx 1.68$, (c) hcp, (d) hcp-like with $\delta/\Phi \approx 1.52$ (see text), (e) $3\square$. The inset of (c) shows a SEM image of the cleft edge.

$2\square$ is very similar to that of $2\triangle$, the transition $2\square \rightarrow 2\triangle$ takes place very rapidly [16], and consequently the rhombic phase appears in a very restricted spatial region of the sample. This is the reason that we do not include the rhombic phase in Fig. 1. The analysis of the $2\triangle \rightarrow 3\square$ transition reveals a rich variety of particle arrangements that look similar to the (100) hcp phase and we call them the 2hcp-like phase. Therefore, the transition sequence is the following: $2\triangle \rightarrow 2$ hcp-like $\rightarrow$2hcp(100) $\rightarrow 2$ hcp-like $\rightarrow 3\square$. The 2 hcp-like phase is very similar to the (100) hcp phase, but with different distance between adjacent string rows. This phase has strong resemblances to the buckling arrangement [1]. Recently, Schöpe *et al.* [8] have described 2*B* and 3*B* phases in wet colloidal crystal thin films, which in fact correspond to the *n* hcp-like phase we are describing here. A closer view of the SEM images shows that the hcp-like phase, as occurs in the buckling phase, can adapt itself to the confined wedge geometry by changing the distance between the adjacent string rows. For the (100) hcp bulk structure, the distance between adjacent rows is $\delta = \sqrt{(8/3)}\Phi = 1.633\Phi$, where Φ is the sphere diameter. However, in our case, one can see that this distance changes from $\delta \approx 1.68\Phi$ [Fig. 1(b)] to $\delta \approx 1.52\Phi$ [Fig. 1(d)]. Simultaneously, optical features in the reflectance also show gradual changes. First, as the system transits between two and three monolayers, a new oscillation period gradually appears. Second, the Bragg diffraction peak absent in the $2\square$ facet clearly emerges at the $2\triangle$ arrangement (at $\lambda = 1.7$ μm). Then, for the 2 hcp-like phase, it shifts to longer wavelength values and smoothly fades out (at around $\lambda = 2.2$ μm) when the light spot approaches the $3\square$ ordering. We have calculated the filling fraction occupied by the spheres in the $2\triangle \rightarrow 3\square$ transition (see Fig. 2). Here we

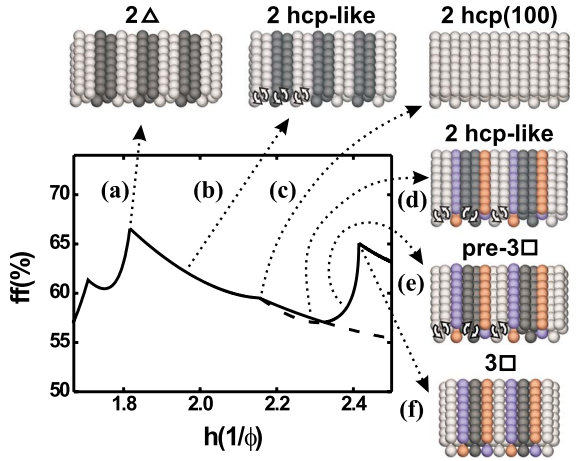

FIG. 2. (Color online) Filling fraction calculation as a function of the reduced cell thickness (h/Φ), Φ being the particle diameter. We also show ordering models to explain how different phases evolve as the cell thickness increases. The different colors in the models identify how microcrystallites rearrange (by rotation) in the facet evolution (see text and the animation movie [16]).

show how the different facets evolve as the cell gap increases. The local maximum at $h/\Phi=1.82$ corresponds to the 2△ phase. As the cell becomes thicker the system smoothly transits to the 2 hcp-like phase. The groups of microcrystallites artificially selected with different colors can help in understanding the transitions between different particle arrangements. The 2△→ 2 hcp-like transition takes place when all microcrystallites rotate around their longer axis (in this case around the [110] direction), thus forming, first, the 2 hcp-like phase [packing model (b) in Fig. 2] and then the 2hcp(100) phase [packing model (c) in Fig. 2]. As the filling fraction value also decreases monotonically, the 2 hcp-like phase is very stable, and, as expected, it can be found in large regions of the sample [16]. An animated movie of the ordering evolution can also be found in the supporting information [16]. The transition 2hcp-(100)→3□ takes place through the 2 hcp-like phase. As the cell thickness increases, the uppermost (lowest) sublayer displaces itself vertically upward (downward) and the rows come closer together. Simultaneously, in order to maximize the filling fraction, the rows from the second and third sublayers approach each other to form the 2 hcp-like phase. Therefore, packing models (b)–(d) from Fig. 2 correspond to SEM images (b)–(d) from Fig. 1. The transition between the 2 hcp-like [packing model (d) in Fig. 2] and the 3□ [packing model (f) in Fig. 2] occurs as follows. In Fig. 2 we have selected different microcrystallite groups. Those with gray colors rotate around the microcrystallite longer axis. Light gray color microcrystallites rotate anticlockwise and those of dark gray color rotate clockwise. Simultaneously, the spheres rows in blue colors are displaced in the direction of the rotation axis, and they approach the confining plates to maximize the filling fraction value. This results in the alignment of all sphere rows in a squared arrangement. The four sublayers from the 2 hcp-like phase rearrange into three sublayers with a square arrangement as the animation movie shows [16]. The transition 2 hcp-like →3□ takes place very rapidly through an

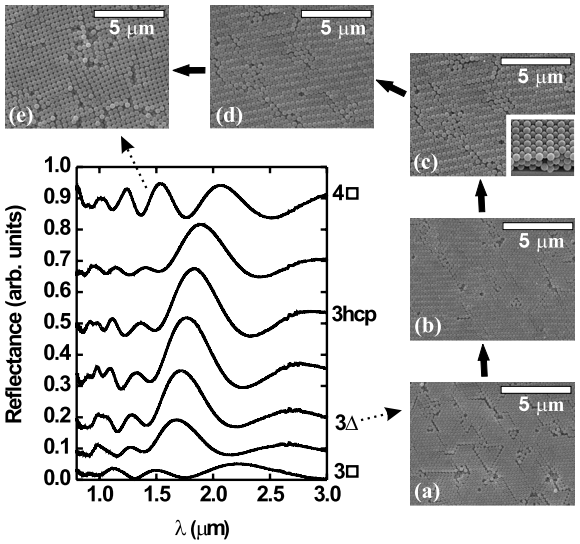

FIG. 3. Reflectance optical spectra obtained over a path for the transition between 3□ and 4□. The sphere diameter being $\Phi=800$ nm. Spectra (shifted for the sake of comparison) show a similar evolution to that shown in Fig. 1. SEM images of the sequence of the different facets: (a) 3△, (b), (c), (d) hcp-like phases, (e) 4□. The inset of (c) shows a SEM image of the cleft edge.

intermediate phase, which we call the pre-3□ [see packing model (e) in Fig. 2]. Figure 4S from the supporting information [16] shows a SEM image of the pre-3□ phase as well as the packing model. The spheres have been colored according to those of the model to help the reader identify this phase. It can be seen how this pre-3□ phase is located between the hcp-like phase and the square phase.

(*b*) 3□→4□ *transition*. Figure 3 shows the optical reflectance spectra as well as SEM images taken on the path transition between the 3□ and 4□ facets, which allow us to characterize the different particle orderings. We have not included the SEM image of the 3□ phase, which has already been shown in Fig. 1(e). Again, as has been described before, the distance between the rows of the 3 hcp-like phase changes gradually when the thickness of the sample increases. The evolution of the optical spectra is very similar to the evolution shown in Fig. 1. The Bragg peak also evolves between $\lambda=1.7$ and 2.2 μm, being a fingerprint of the evolution of the interlayer spacing in the transition between 3□ and 4□ monolayers. The model of the transition 3 hcp-like →4□ is very similar to the model described in Fig. 2. Therefore the transition sequence is the following: 3△→3 hcp-like→3hcp(100)→3 hcp-like→4□.

The hcp-like phase we have shown so far also appears for

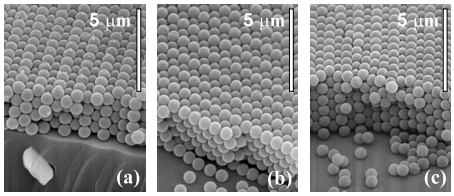

FIG. 4. SEM images of hcp-like phase for (a) 4, (b) 5, and (c) 6 ML.

thicker colloidal films. Figure 4 shows hcp-like layering in the case of four, five, and six monolayers. Indeed these phases appear in large zones of the wedge cell. As the interlayer distance of the hcp-like phase can easily be adapted to be commensurate to the wedge thickness, it can easily be found in large areas of the sample. This is proof of the stability of this phase.

To summarize, we have shown that the hcp-like phase appears in the transition $n\triangle \rightarrow (n+1)\square$ in large surfaces areas because of its ability to reorganize itself according to the changing contour conditions imposed by the wedge type geometry. More importantly, it gives a unified understanding of how the system smoothly transits between different particle orderings when the thickness value changes gradually.

We would like to thank A. Moreno for her help in the sample processing, and the Electronic Microscopy Service from the Polytechnic University of Valencia for the SEM characterization. This work has been partially supported by the Spanish CICyT (Project No. MAT2006-03097). I.R. thanks the Spanish Ministry of Education and Science for support.

[1] P. Pieranski, L. Strzelecki, and B. Pansu, Phys. Rev. Lett. **50**, 900 (1983).
[2] J. H. Conway and N. J. A. Sloane, *Sphere, Packings, Lattices, and Groups* (Springer, New York, 1993).
[3] S. M. Ilet, A. Orrock, W. C. K. Poon, and P. N. Pusey, Phys. Rev. E **51**, 1344 (1995).
[4] B. Pansu, Pi. Pieranski, and Pa. Pieranski, J. Phys. (Paris) **45**, 331 (1984).
[5] S. Neser, C. Bechinger, P. Leiderer, and T. Palberg, Phys. Rev. Lett. **79**, 2348 (1997).
[6] D. H. Van Winkle and C. A. Murray, Phys. Rev. A **34**, 562 (1986).
[7] A. Barreira Fontecha, H. J. Schöpe, H. König, T. Palberg, R. Messina, and H. Löwen, J. Phys.: Condens. Matter **17**, S2779 (2005).
[8] H. J. Schöpe, A. Barreira Fontecha, H. König, J. Marques Hueso, and R. Biehl, Langmuir **22**, 1828 (2006).
[9] M. Schmidt and H. Löwen, Phys. Rev. Lett. **76**, 4552 (1996).
[10] R. Zangi and S. A. Rice, Phys. Rev. E **61**, 660 (2000).
[11] H. K. Bock, E. Gubbins, and K. G. Ayappa, J. Chem. Phys. **122**, 094709 (2005).
[12] T. Chou and D. R. Nelson, Phys. Rev. E **48**, 4611 (1993).
[13] A. Fortini and M. Dijkstra, J. Phys.: Condens. Matter **18**, L371 (2006).
[14] F. Ramiro-Manzano, F. Meseguer, E. Bonet, and I. Rodriguez, Phys. Rev. Lett. **97**, 028304 (2006).
[15] Y. Lu, Y. Yin, B. Gates, and Y. Xia, Langmuir **17**, 6344 (2001).
[16] See EPAPS Document No. E-PLEEE8-76-R02711 for additional images and a movie. For more information on EPAPS, see http://www.aip.org/pubservs/epaps.html.